Journal of Holistic Integrative Pharmacy 6 (2025) 41–49

Contents lists available at ScienceDirect

Journal of Holistic Integrative Pharmacy

journal homepage: www.keaipublishing.com/en/journals/journal-of-holistic-integrative-pharmacy

Preparation of TPM–NCs–gel and its effect on subcutaneous abscess caused by *Staphylococcus aureus*

Quanwei Xie [a,1], Feirong Zhou [a,1], Runan He [a], Lianbao Ye [a], Zonghao Lin [a], Xiangyu Nie [a], Yuanzheng Wei [b,*], Chuqin Yu [a,**]

[a] *Centre for Drug Research and Development, Guangdong Pharmaceutical University/Guangdong Provincial Key Laboratory of Advanced Drug Delivery Systems/ Guangdong Provincial Engineering Center of Topical Precise Drug Delivery System, Guangzhou, 510006, China*
[b] *Guangdong Provincial Biotechnology Research Institute (Guangdong Laboratory Animal Monitoring Center), Guangzhou, 510663, China*

ARTICLE INFO

Keywords:
TPM
Nanocrystal
Gel
Staphylococcus aureus
Subcutaneous abscess

ABSTRACT

Objective: The insoluble compound 1,1′-(2,4,6-trihydroxy-1,3-phenylene)bis(3-methylbutan-1-one) (TPM) is used in preparing a TPM nanocrystals gel (TPM–NCs–gel), and its *in vitro* antibacterial activity and therapeutic effect on subcutaneous abscesses caused by *Staphylococcus aureus* were evaluated.
Methods: The effect of a prescription technology on the particle size of a TPM–NCs suspension was investigated using a single factor, and the TPM–NCs prescription was optimized using a Box–Behnken design. A TPM–NCs–gel was prepared using hydroxyethyl cellulose–HHX (HEC–HHX) as a gel matrix and characterized. The minimum inhibitory concentration (MIC) and minimum bactericidal concentration (MBC) of TPM–NCs–gel were determined with the microdilution method. The susceptibility of *Staphylococcus aureus* to mupirocin ointment, TPM–NCs–gel, and TPM–gel was evaluated by the disk diffusion method. The efficacy of the TPM–NCs–gel for subcutaneous abscess caused by *Staphylococcus aureus* was evaluated using a mouse model.
Results: The optimized TPM–NCs prescription consisted of Tween 80 and TPGS (2.47%), TPM (1.24%) and mannitol (2.32%). The size of the TPM–NCs was 98.2 ± 3.9 nm, and the polydispersion coefficient (PDI) was 0.235 ± 0.023. The particle size and PDI of the TPM–NCs–gel were 112.4 ± 7.3 nm and 0.148 ± 0.068, respectively. The MIC and MBC were both 2.98 μg/mL. After 12 days of administration, the bacteria in the abscess site of 2% TPM–NCs–gel experimental group were cleared, the inflammatory cells were reduced, and the skin structure was remodeled.
Conclusion: After TPM was prepared into TPM–NCs–gel, the antibacterial activity was enhanced, *Staphylococcus aureus* at the site of abscess was effectively removed, and wound healing was promoted.

1. Introduction

Staphylococcus aureus is the most common gram-positive pathogen in clinical practice, and it easily colonizes the skin and mucosal surfaces of humans and animals.[1,2] The selection pressure exerted by the irregular use and abuse of antibiotics on bacteria and other pathogens has promoted the evolution of bacteria's protective mechanisms, such as resisting the action of antibiotics through inactivation, elimination, or other means. These mechanisms enabled the bacteria to continuously grow and reproduce, generating drug-resistant strains. Antibiotic resistance and lack of effective vaccines complicate the treatment of *Staphylococcus aureus* infections.[3–5] According to the World Health Organization, at least 700,000 patients die from diseases caused by drug-resistant bacteria every year. Thus, safe and efficient antibacterial drugs are urgently needed.[6]

Phloroglucinol compounds constitute a class of compounds with the phloroglucinol as the basic parent nucleus and widely exist in more than 200 plants in nature, which exert strong bactericidal effects, demonstrating great development potential and application value.[7–9] With the mature technology of active ingredient screening and total synthesis,

* Corresponding author.
** Corresponding author.
E-mail addresses: yzwei87@163.com (Y. Wei), pn333@163.com (C. Yu).
Peer review under the responsibility of Editorial Board of Journal of Holistic Integrative Pharmacy.
[1] These authors contributed equally to this manuscript and worked as co-first authors.

https://doi.org/10.1016/j.jhip.2025.02.004
Received 26 December 2024; Received in revised form 19 February 2025; Accepted 20 February 2025

people have modified the active groups of active ingredients of natural products, and synthesized a large number of compounds with good pharmacological activity, strong stability, and low toxic side effects by a simple and easy method.

1,1′-(2,4,6-trihydroxy-1,3-phenylene) bis (3-methylbutan-1-one) (TPM) belongs to a new fully synthetic compound category designed with phloroglucinol as the parent core. Previous studies found that TPM showed excellent antibacterial activity against *Staphylococcus aureus in vitro*, which is close to vancomycin, and can effectively remove methicillin-resistant *Staphylococcus aureus* from mouse wounds, promote wound healing, and have good biosafety *in vivo*.[10] However, TPM has poor water solubility, which will affect its effect as it is difficult to penetrate the skin barrier for external use. It is supposed that preparing it into nano preparations will contribute to improving its solubility and bioavailability.

In drug development, many candidate drugs are insoluble in water, thus showing low bioavailability and poor absorption effects.[11,12] Preparing insoluble candidate drugs into Nanocrystals (NCs) is one of the effective ways to improve its solubility.[13] NCs have small particle size, large specific surface areas, and high drug loads (require less amounts of carrier materials than other carriers), and are easy to industrialize.[14,15] These features not only enhance adhesion to biofilms but also improve the solubility of drugs, thereby improving bioavailability.[16] However, TPM–NCs suspensions have poor stability, and thus surfactants, polymers, or buffer antifreeze agents are added to stabilize NCs.[17,18] In addition, NCs suspensions are difficult to retain in the skin, and thus TPM–NCs–gel was prepared to offset poor moisture retention, high fluidity, and weak retention ability. In this study, the *in vitro* antibacterial activity and the therapeutic effect on subcutaneous abscess induced by *Staphylococcus aureus* in mice were assessed for TPM–NCs–gel, with the aim to provide experimental data for the subsequent development and application of TPM.

2. Materials and methods

2.1. Materials

Healthy SPF grade KM mice, half male and half female, weight: 20 ± 2 g, the license number of animal: SYXK (Guangdong) 2023-0318, ethical committee: (Institutional Animal Care and Use Committee, Guangzhou Boyao Biosciences Co., Ltd.); TPM (purity 98.88%, provided by Professor Ye Lianbao's research group); Tween 80 (Shanghai McLean Biochemical Technology Co., LTD.); Vitamin E polyethylene glycol succinate (TPGS, Shanghai Lianlu Industrial Co., LTD.); Hydroxypropyl Methyl Cellulose (HPMC, Dow Chemical Company, USA); HEC–HHX (Ashland, USA); Poloxamer 188 (P 188, Beijing Fengli Jingqiu Trading Co., LTD.); Polyvinyl alcohol 1788 (PVA 1788, Shanghai Aladdin Biochemical Technology Co., LTD.); Polyvinylpyrrolidone k30 (PVP k30, Beijing Fengli Jingqiu Trading Co., LTD.); Mannitol (Merck GMBH, Germany); Propylene glycol (Guangdong Pengyuan Chemical Co., LTD.); Disodium EDTA (EDTA–2Na, Tianjin Zhiyuan Chemical Reagent Co., LTD.); Triethanolamine (Tianjin Zhiyuan Chemical Reagent Co., LTD.); Methyl paraben (Yancheng Baike Chemical Industry Company); Ethyl paraben (Tianjin Zhiyuan Chemical Reagent Co., LTD.); Phosphoric acid (Tianjin Zhiyuan Chemical Reagent Co., LTD.); Glycerin (Guangdong Pengyuan Chemical Co., LTD.); Transcutol P (GATTEFOSSE Co., LTD.); Nutrition AGAR (Guangdong Huankai Microbial Technology Co., LTD.); LB broth (Guangdong Huankai Microbial Technology Co., LTD.); Blank drug-sensitive paper (Zhuhai Gete Biotechnology Co., LTD.); Sterile TTC solution (Guangdong Huankai Microbial Technology Co., LTD.); *Staphylococcus aureus* (Shanghai Yingxin Laboratory Equipment Co., LTD.); PBS buffer (Thermo Fisher Technology (China) Co., LTD.); Saline (Sichuan Kelun Pharmaceutical Co., LTD.); Vitin Hair Removal Cream (Reckitt Benckiser (China) Co., LTD.); Mupirocin ointment (Sino-American Tianjin Schix Pharmaceutical Co., LTD.); 4% paraformaldehyde (White Shark Biotechnology Co., LTD.); Sutai (France Vick GMBH); TPM-NCs-gel (self-develop).

2.2. Chromatographic conditions and solution preparation

An Agilent ZORBAX SB–C8 (4.6 mm × 150 mm, 5 μm) column with a mobile phase consisting of methanol–0.1% phosphoric acid aqueous solution (75:25) was used. The detection wavelength was set at 274 nm, the flow rate was 1.0 mL/min, and the column temperature was 30 °C. The sample size was 10 μL. The detector was an ultraviolet absorption photodetector.

Test product solution: TPM–NCs–gel (1.0 g) was placed in a 10 mL volumetric bottle. After the mobile phase was added, the gel was ultrasonicated for 5 min to a constant volume and agitated until a test product reserve solution was obtained. The reserve liquid (1 mL) was removed and transferred to a 5 mL volumetric bottle, mixed with the mobile phase, and ultrasonicated for 5 min. A constant volume was obtained, and the mixture was shaken well and filtered with a 0.22 μm microporous filter membrane to yield the test solution.

Control product solution: Exactly 10 mg of TPM was placed in a 10 mL volumetric bottle, mixed with the mobile phase to constant volume, ultrasonicated for 5 min, shaken well, and filtered with a 0.22 μm microporous filter membrane to yield a control product reserve solution. The reserve liquid (1 mL) was added to a 5 mL volumetric bottle, mixed with a mobile phase to constant volume, ultrasonicated for 5 min, shaken well, and filtered with a 0.22 μm microporous filter membrane to yield the control solution.

2.3. Determination of TPM oil and water distribution coefficient (log P)

The oil–water distribution coefficient of TPM was determined using the shaker method.[19] *n*-Octanol was mixed with water and solutions of different pH in a ratio of 1:9. After constant temperature oscillation for 24 h in a 37 °C constant-temperature oscillator, the mixture was transferred to a liquid separation funnel. After the solution was layered, the upper water–saturated *n*-octanol solution and the lower layer *n*-octanol–saturated aqueous solution were prepared.

Excess TPM was weighed and added to a water-saturated *n*-octanol solution, ultrasonicated until TPM no longer dissolved, and centrifuged at 10,000 rpm/min for 15 min. The supernatant was collected, diluted with the mobile phase, and filtered with the 0.22 μm microporous filter membrane. Then, the initial concentration (C_o) of TPM in saturated *n*-octanol was calculated according to the chromatographic conditions described in Section 2.2. A solution containing a TPM-saturated *n*-octanol solution and an *n*-octanol saturated aqueous solution in a ratio of 1:9 was prepared and placed in a 37 °C constant-temperature oscillator for 48 h. The upper solution was centrifuged at a speed of 10,000 rpm/min for 15 min, the supernatant was collected, and the flow phase was diluted. A 0.22 μm microporous filter membrane was used, and the chromatographic conditions described in Section 2.2 were used. The sample was measured, and the concentration C_{ow} of TPM after the two-phase distribution equilibrium was calculated. The log P of TPM was calculated using the formula as follows:

$$\text{Log P} = \text{Log } C_o/C_w = \text{Log } C_o/(C_o\text{-}C_{ow})$$

2.4. Measurement of TPM equilibrium solubility

Excess TPM was transferred to a test tube, mixed with different solvents, oscillated in a 37 °C constant-temperature oscillator for 24 h, and removed. The sample solution was placed at room temperature and centrifuged at 10,000 rpm/min for 15 min, and the supernatant was collected, filtered with a 0.22 μm microporous filter membrane, and then injected for analysis under the chromatographic conditions described in Section 2.2. The equilibrium solubility of TPM in different solvents was calculated.

2.5. Preparation of TPM–NCs

2.5.1. Preparation process

Nipergin methyl ester and nipogin ethyl ester were placed in hot water (90 °C), and HPMC was slowly dispersed in hot water, placed in an area with room temperature, and stirred until it was fully swollen. Then, surfactants (TPGS and Tween 80) were added. The mixture was stirred until HPMC was dissolved (38 °C water bath). TPM was added at room temperature. The resulting mixture was dispersed evenly and subjected to 5000 rpm/min high-speed shear for 5 min with an 80-mesh sieve after high-pressure homogenization. Mannitol was added, and the mixture was stirred evenly to yield a TPM–NCs suspension.

2.5.2. Single-factor inspection

The prepared suspension was investigated at different shear speeds (3000, 5000, and 7000 rpm/min), shear times (3, 5, and 7 min), and homogeneous pressure (1500, 1700, and 1900 bar), and homogenization was performed 20, 30, and 40 times. The prescription processes were unchanged, and the influence of the process on the particle size of TPM–NCs was examined.

Different types of surfactants (Tween 80; P188; TPGS; Tween 80 and P188; P188 and TPGS; Tween 80 and TPGS), compounding ratios of surfactants (TPGS: Tween 80 = 1:1, 2:1, 3:1), surfactant dosages (1.0%, 2.0%, and 3.0%), stabilizers (HPMC, PVA 1788, and PVP k30), stabilizer dosages (0.3%, 0.5%, and 0.8%), drug loads (1.0%, 1.5%, 2.0%, and 3.0%), and mannitol dosages (0.0%, 2.0%, 4.0%, 6.0%, and 8.0%) were used, and the prescription processes were unchanged. After mannitol was added (when a solution was homogeneous or after homogenization), the effect of the prescription processes on the particle size of TPM–NCs was investigated.

2.5.3. Response surface design–optimized TPM–NCs formulation

According to the results of the single-factor test, three factors were selected, namely, the surfactant dosage (A), drug load (B), and mannitol dosage (C), and three levels were set for each factor. The particle size of TPM–NCs was used as the evaluation index, and Design-Expert software was used to optimize the TPM–NCs formulation.

2.5.4. Prescription process verification test

According to the best prescription obtained by model fitting described in Section 2.5.3, the formulation was verified, three batches of TPM–NCs were prepared in parallel, and the particle size and PDI of the TPM–NCs were measured.

2.6. Preparation and characterization of the TPM–NCs–gel

The TPM–NCs suspension prepared according to the formulation described in Section 2.5.3 was mixed with 0.2% EDTA–2Na and 1.4% HEC–HHX, and the mixture was stirred for approximately 30 min. After HEC–HHX was fully swollen, 12% transcutol P and 5% glycerol were added, and the mixture was stirred. The TPM–NCs–gel was obtained by adjusting pH to approximately 6.0 with triethanolamine and then characterized. The strength, hardness, and adhesion value of the gel were measured with a texture analyzer. The single-pressure analysis mode was selected, the probe model was a P/0.5 cylinder, and the experimental parameter was set at a pretest velocity of 1.5 mm/s. The speed during and after test was 1.0 mm/s, the compression distance is 5 mm, and the trigger force was 1.0 g. An appropriate amount of blank gel and TPM–NCs–gel were mixed in a test cup, the position of the test cup was adjusted so that it was directly under the probe of the texture analyzer, and the test results were recorded in parallel three times.

2.7. Determination of MIC and MBC

TPM–NCs–gel and TPM–gel were diluted with LB broth to yield TPM concentrations of 47.60, 23.80, 11.90, 5.95, 2.98, 1.49, and 0.74 μg/mL. A blank control group and a negative control group were established in each group. A TTC solution (10 μL) was cultured in a constant-temperature incubator at 37 °C for 24 h and then added to each well. After 2 h of culturing, the color of the solution did not change, indicating that no bacteria survived, that is, MIC. Bacterial suspensions (10 μL) with concentrations of MIC, 2MIC, and 4MIC were collected and inoculated into a solid medium with the scriber method. After 24 h of culturing, the number of colonies was less than five after treatment with corresponding drugs at the lowest concentration, that is MBC.[20,21]

2.8. Determination of bacteriostatic zone

The concentrations of mupiroxacin ointment and TPM–gel were diluted to 100 μg/mL with LB broth, and the concentrations of TPM–NCs–gel were diluted to low, medium, and high (25, 50, and 100 μg/mL). The blank gel was diluted with LB broth as a negative control. Mupirocin ointment (10 μL), TPM–NCs–gel, TPM–gel, and blank gel diluent were added to a drug-sensitive paper, dried, and set aside.

A bacterial suspension (100 μL; 1.5×10^8 CFU/mL) was uniformly coated in a solid medium, and drug-sensitive tablets were added. After 24 h of inverted culture, the diameter of the antibacterial zone was measured. The experiment was repeated three times for each group.

2.9. In vivo antimicrobial test

After 5 days of adaptive feeding, the back hair of each mouse was removed, and the mice were injected with 50 μL (1.5×10^8 CFU/mL) of bacterial suspension under the skin at its hair removal site. After 24 h of infection, the modeling was considered successful when suppurative lesions appeared at the hair-removal area. After the successful construction of the model, blank gel was administered to the model group, 0.5%, 1.0%, and 2.0% TPM–NCs–gel to the experimental group, and Mupirocin ointment to the positive group once in the morning and once in the evening. Changes in the body weight of the mice were observed and recorded. After 3, 7, and 12 days of treatment, the skin in the lesion site was obtained, the bacterial load in the abscess was recorded, the skin tissue was sliced for H&E and Masson staining, and tissue changes in the lesion site were observed. The animal experiment was approved by the Animal Ethical Committee of Guangzhou Boyao Biotechnology Co. LTD. (IAEC-K-231212-03).

2.10. Statistical analysis

All statistical analyses were performed using the Statistical Product and Service Solutions (SPSS) 22.0 and GraphPad Prism version 6.0. All data are expressed as mean ± SD and evaluated by analysis of variance (ANOVA).

3. Results

3.1. TPM oil-water distribution coefficient

As shown in Table 1.

Table 1
The oil-water distribution coefficient of TPM.

System	Log P
n–Octyl alcohol–Water	0.868
n–Octyl–hydrochloric acid (pH = 1.2)	1.239
n–Octyl–ABS buffer (pH = 4.5)	1.646
n–Octyl–PBS buffer (pH = 6.8)	1.147
n–Octyl–PBS buffer (pH = 7.2)	1.254

3.2. TPM equilibrium solubility

As shown in Table 2.

3.3. TPM–NCs single-factor investigation results

3.3.1. Shear speed

At shear speeds of 3000, 5000, and 7000 rpm/min, the particle sizes were found to be 473.2 ± 15.6, 311.0 ± 8.1, and 428.3 ± 30.4 nm, respectively. Similarly, the PDI values were determined to be 0.216 ± 0.014, 0.290 ± 0.020, and 0.192 ± 0.010, respectively. Our observations indicated that an increase in shear speed initially reduced the particle size of the TPM–NCs. However, beyond a certain threshold, further increases in speed lead to an increase in particle size. Consequently, a shear speed of 5000 rpm/min was chosen for the subsequent experiment.

3.3.2. Shear time

At shear times of 3, 5, and 7 min, the particle sizes were found to be 418.4 ± 10.3, 311.0 ± 8.1, and 357.0 ± 43.0 nm, respectively. Similarly, the PDI values were determined to be 0.192 ± 0.004, 0.290 ± 0.020, and 0.218 ± 0.031, respectively. Our observations indicated that when shear time was extended to a certain period, the effect of the shear time on the particle size was not obvious. Consequently, a shear time of 5 min was chosen for the subsequent experiment.

3.3.3. Homogenization pressure

At homogenization pressures of 1500, 1700, and 1900 bar, the particle sizes were found to be 559.8 ± 18.1, 487.7 ± 25.8, and 311.0 ± 8.1 nm, respectively. Similarly, the PDI values were determined to be 0.232 ± 0.006, 0.213 ± 0.012, and 0.290 ± 0.020, respectively. Our observations indicated that particle sizes of the TPM–NCs decreased with increasing homogenization pressures. Consequently, homogenization pressure of 1900 bar was chosen for the subsequent experiment.

3.3.4. Homogenization times

At homogenization times of 20, 30, and 40, the particle sizes were found to be 563.7 ± 4.5, 311.0 ± 8.1, and 295.6 ± 12.1 nm, respectively. Similarly, the PDI values were determined to be 0.242 ± 0.002, 0.290 ± 0.020, and 0.227 ± 0.053, respectively. Our observations indicated that when homogenization times were extended to a certain period, the effect of the homogenization times on the particle size was not obvious. Consequently, the homogenization time of 30 was chosen for the subsequent experiment.

3.3.5. Surfactant screening

When the surfactant is Tween 80, P 188, TPGS, (Tween 80 and P 188), (Tween 80 and TPGS), and (TPGS and P 188), the particle sizes were found to be 311.0 ± 8.1, 1535.0 ± 50.5, 575.9 ± 33.7, 989.3 ± 8.4, 460.1 ± 24.7, and 932.5 ± 38.8 nm, respectively. Similarly, the PDI values were determined to be 0.290 ± 0.020, 0.407 ± 0.021, 0.242 ± 0.013, 0.330 ± 0.09, 0.209 ± 0.013, and 0.312 ± 0.013, respectively. TPGS has many excellent properties, being used as a solvent enhancer and stabilizer, and improving the *in vitro* osmotic promotion efficiency of drugs. Consequently, (Tween 80 and TPGS) were chosen for the subsequent experiment.[22,23]

3.3.6. Screening of surfactant mix ratio

At TPGS:Tween 80 = 1:1, 2:1, and 3:1, the particle sizes were found to be 460.1 ± 24.7, 572.2 ± 21.7, and 712.0 ± 78.1 nm, respectively. Similarly, the PDI values were determined to be 0.209 ± 0.013, 0.250 ± 0.009, and 0.301 ± 0.029, respectively. Our observations indicate that increasing the use ratio of TPGS prevents reduction in the particle size of TPM–NCs. Consequently, TPGS:Tween 80 = 1:1 was chosen for the subsequent experiment.

3.3.7. Screening of surfactant dosage

When the surfactant dosages are 1.0%, 2.0%, and 3.0%, the particle sizes were found to be 460.1 ± 24.7, 53.6 ± 1.0, and 40.9 ± 0.3 nm, respectively. Similarly, the PDI values were determined to be 0.209 ± 0.013, 0.276 ± 0.014, and 0.243 ± 0.015, respectively. Consequently, the surfactant dosage of 3.0% was chosen for the subsequent experiment.

3.3.8. Screening of stabilizer

At stabilizer PVP k30, PVA 1788, and HPMC, the particle sizes were found to be 63.7 ± 6.0, 110.3 ± 15.1, and 40.9 ± 0.3 nm, respectively. Similarly, the PDI values were determined to be 0.282 ± 0.030, 0.437 ± 0.062, and 0.243 ± 0.015, respectively. Consequently, HMPC was chosen as the stabilizer for the subsequent experiment.

3.3.9. Screening of stabilizer dosage

At stabilizer dosages of 0.3%, 0.5%, and 0.8%, the particle sizes were found to be 38.6 ± 0.3, 40.9 ± 0.3, and 43.4 ± 0.5 nm, respectively. Similarly, the PDI values were determined to be 0.341 ± 0.025, 0.243 ± 0.015, and 0.215 ± 0.010, respectively. Consequently, the stabilizer dosage of 0.5% was selected for the subsequent experiment.

3.3.10. Screening of drug load

At the drug load of 1.0%, 1.5%, 2.0%, and 3.0%, the particle sizes were found to be 40.9 ± 0.3, 71.4 ± 2.1, 255.1 ± 7.1, and 355.1 ± 3.2 nm, respectively. Similarly, the PDI values were determined to be 0.243 ± 0.015,0.260 ± 0.019, 0.132 ± 0.004, and 0.174 ± 0.007, respectively. Our observations indicated that the particle size of the TPM–NCs

Table 2
The solubility of TPM in different solvents.

Solvent	Solubility (mg/mL)
75% Carbinol	3.56
50% Carbinol	0.52
30% Carbinol	Almost insoluble
75% Ethyl alcohol	4.56
50% Ethyl alcohol	2.67
30% Ethyl alcohol	0.20
Purified water	Almost insoluble
Normal saline	Almost insoluble
Hydrochloric acid (pH = 1.2)	Almost insoluble
ABS buffer (pH = 4.5)	Almost insoluble
PBS buffer (pH = 6.8)	Almost insoluble
PBS buffer (pH = 7.2)	Almost insoluble
1.0% Tween 80	5.71
1.5% Tween 80	5.78
2.0% Tween 80	5.25
0.6% SDS	0.45
0.8% SDS	0.71
1.0% SDS	0.96

Table 3
Test design and results.

No.	A: Surfactant dosage (%)	B: Drug load (%)	C: Mannitol dosage (%)	Particle size (nm)
1	1.00	1.00	3.00	478.5
2	1.00	1.25	0	481.7
3	1.90	1.25	3.00	201.8
4	1.90	1.25	3.00	190.5
5	1.90	1.50	6.00	320.2
6	1.90	1.25	3.00	180.2
7	2.80	1.50	3.00	181.4
8	2.80	1.25	0	121.0
9	1.90	1.00	6.00	277.4
10	1.90	1.25	3.00	187.4
11	1.00	1.25	6.00	398.5
12	2.80	1.25	6.00	113.4
13	1.00	1.50	3.00	393.3
14	1.90	1.50	0	371.1
15	1.90	1.25	3.00	183.8
16	1.90	1.00	0	316.7
17	2.80	1.00	3.00	41.0

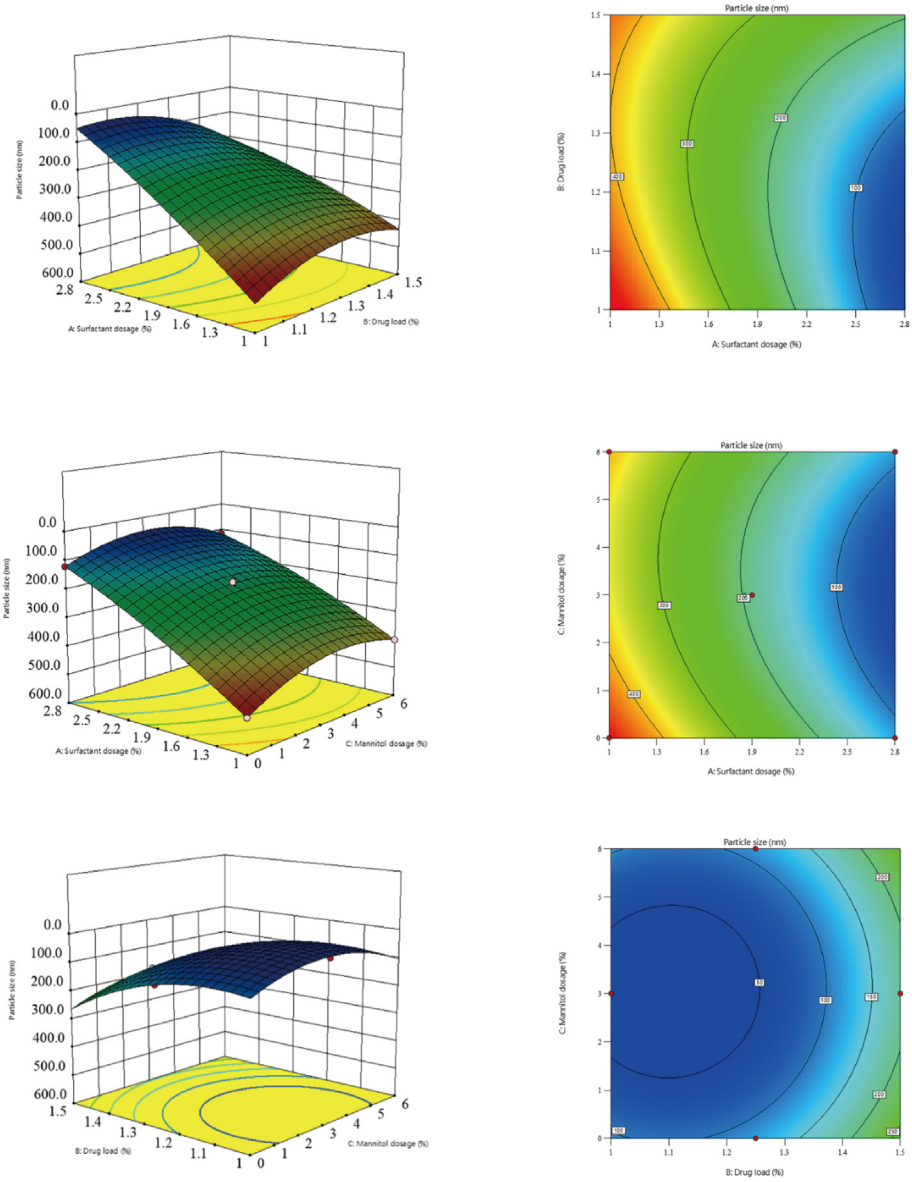

Fig. 1. 3D diagram and isoline diagram of response surface.

Table 4
Particle size and PDI of TPM–NCs ($n = 3$).

Lot No.	Particle size (nm)	PDI
2023092401	98.2 ± 3.9	0.235 ± 0.023
2023092402	97.5 ± 1.6	0.242 ± 0.006
2023092403	98.8 ± 1.1	0.226 ± 0.011

suspension gradually increased with drug proportion. Consequently, the drug load of 1.5% was selected for the subsequent experiment.

3.3.11. *Screening of mannitol dosage*

At the mannitol dosages of 0.0%, 2.0%, 4.0%, 6.0%, and 8.0%, the particle sizes were found to be 352.7 ± 3.8, 129.9 ± 7.3, 136.2 ± 49.5, 87.5 ± 12.7, and 71.4 ± 2.1 nm, respectively. Similarly, the PDI values were determined to be 0.175 ± 0.003, 0.229 ± 0.013, 0.161 ± 0.065, 0.225 ± 0.069, and 0.260 ± 0.019, respectively. Our observations

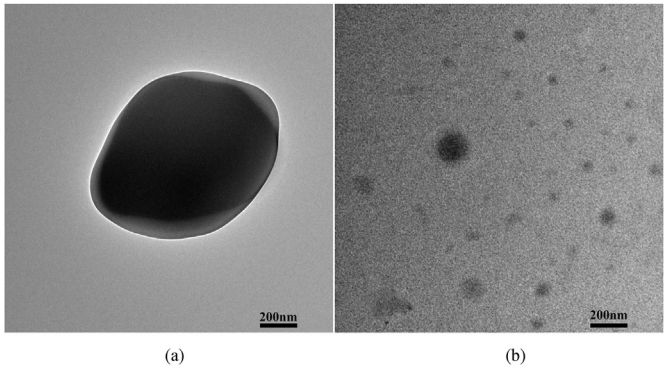

(a) (b)

Fig. 2. Transmission electron micrograph of TPM (a) and TPM–NCs-gel (b) (× 20000).

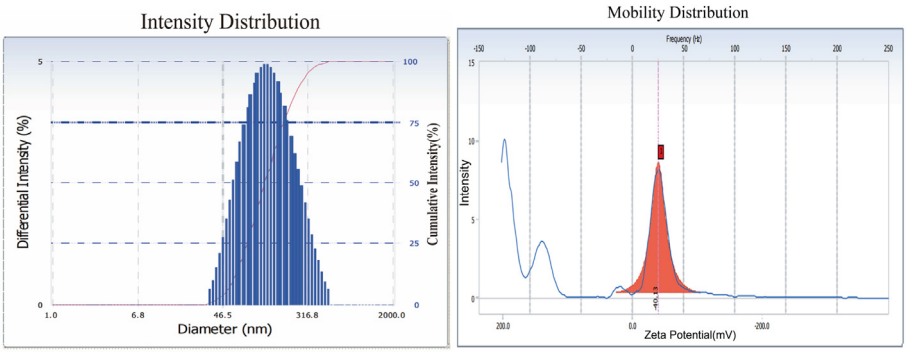

Fig. 3. Particle size (a) and Zeta potential diagram (b) of TPM–NCs–gel.

indicated that when the dosage of mannitol increased to 6.0%, the influence of mannitol on the particle size of the TPM–NCs decreased. Consequently, the dosage of mannitol of 6.0% was selected for the subsequent experiment.

3.3.12. Investigation of adding method of mannitol

The particle size of the TPM–NCs obtained by adding mannitol after homogenization was 87.5 ± 12.7 nm, and PDI was 0.225 ± 0.069. The particle size of the TPM–NCs obtained by adding mannitol when homogenization was 630.2 ± 66.3 nm, and PDI was 0.297 ± 0.017. Thus, the TPM–NCs were prepared by adding mannitol after homogenization.

3.4. Response surface method optimization

The experimental design and results are shown in Table 3. By fitting and analyzing the experimental data, the optimal fitting model and equation of response value Y (particle size, nm) for independent variables were obtained: $Y = 188.74 - 161.90A + 19.05B - 22.63C + 56.40AB + 18.90AC - 2.90BC + 21.06A^2 + 63.75B^2 + 68.85C^2$. The correlation coefficient of the model R^2 was 0.9982, indicating the good fit of the equation. The 3D and contours of the response surface are shown in Fig. 1. The optimal prescription obtained through analysis of response surface was as follows: surfactant dosage, 2.47%; drug load, 1.24%; and mannitol dosage, 2.32%. The particle size of TPM–NCs predicted by the model is 98.8 nm.

3.5. Validation test

The experimental results are shown in Table 4. The particle size of TPM–NCs was close to the predicted value (98.8 nm), indicating that the optimized formulation was feasible.

3.6. TPM–NCs–gel characterization

3.6.1. Microstructure

As shown in Fig. 2, TPM had an irregular shape and large particle size, whereas TPM–NCs-gel had a small particle size and was circular with uniform distribution. The particle sizes of TPM and TPM-NCs-gel were 1012.1 ± 99.7 and 106.5 ± 13.9 nm, respectively.

3.6.2. Particle size distribution and Zeta potential

After the TPM–NCs–gel was diluted 100 times, the particle size, the polydispersion coefficient (PDI), and potential of the gel were measured with DelsaNano and a potentiometer in parallel three times. The results are shown in Fig. 3. The particle size of TPM in TPM–NCs–gel was 112.4 ± 7.3 nm, the PDI was 0.148 ± 0.068, and the Zeta potential was −38.60 ± 2.03 mV.

3.6.3. Determination of pH

An appropriate amount of TPM–NCs–gel was collected, and its pH was determined, and the pH was measured in parallel three times at room temperature. The measured pH value is 6.35 ± 0.01, which meets the requirements of skin topical preparation.

3.6.4. Centrifugal stability

An appropriate amount of TPM–NCs–gel was transferred to a centrifuge tube and centrifuged at 5000 rpm/min for 20 min. The state of the

Table 5
Texture properties of gel ($n = 3$).

Sample	Strength (g)	Hardness (g)	Adhesion value (g/s)
Blank gel	3.686 ± 0.097	4.074 ± 0.100	2.893 ± 0.432
TPM–NCs–gel	3.581 ± 0.059	3.846 ± 0.037	2.366 ± 0.373

Table 6
Measurement results of MIC ($n = 6$) and MBC ($n = 3$).

Sample	MIC (μg/mL)	MBC (μg/mL)
TPM–NCs–gel	2.98	2.98
TPM-gel	11.90	11.90

Table 7
Measurement results of the bacteriostatic zone ($n = 3$).

Sample	Bacteriostatic zone (mm)
TPM–gel (100 μg/mL)	6.71 ± 0.13
TPM–NCs–gel (25 μg/mL)	6.76 ± 0.97
TPM–NCs–gel (50 μg/mL)	9.10 ± 0.33**
TPM–NCs–gel (100 μg/mL)	14.16 ± 0.91****
Mupirocin ointment (100 μg/mL)	20.70 ± 0.45****

Note: $^{**}P < 0.01$, $^{****}P < 0.0001$, compare to the TPM-gel group.

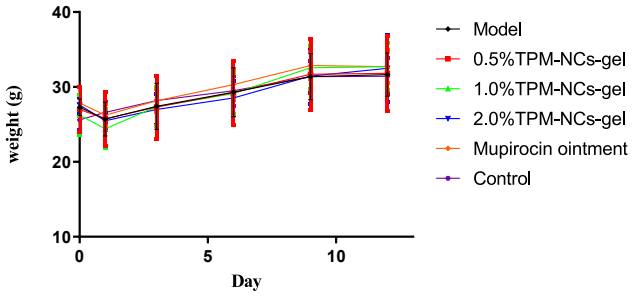

Fig. 4. The trend curve of mice weight ($n = 6$).

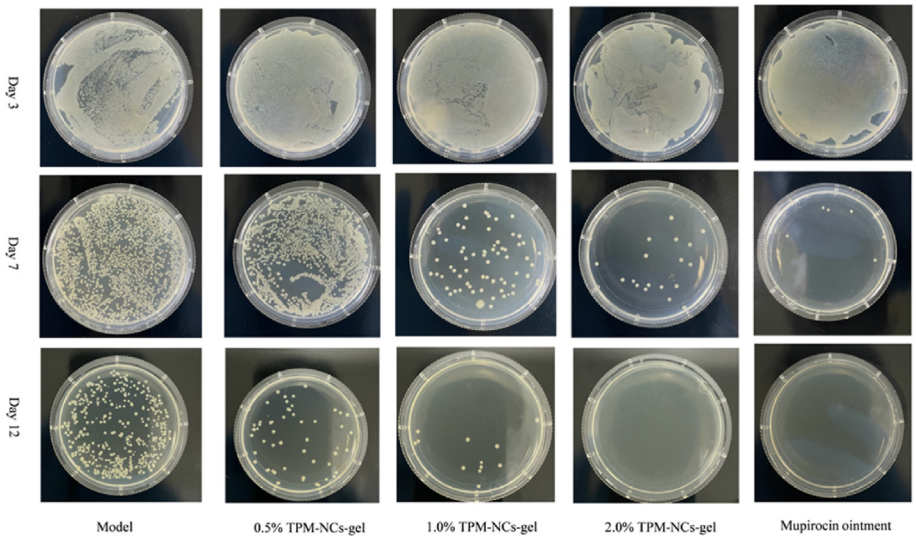

Fig. 5. Picture of colonies formed on agar plates from mice skin extracts.

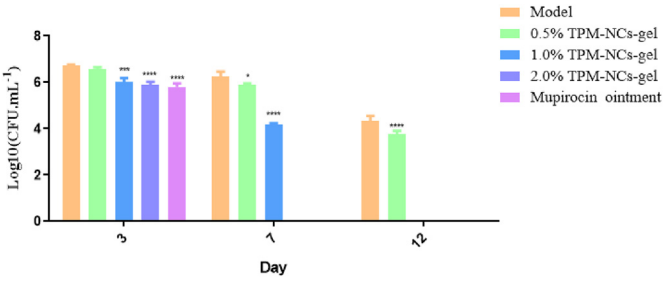

Fig. 6. Skin bacterial load in mice ($n = 3$). $^{*}P < 0.5$, $^{***}P < 0.001$, $^{****}P < 0.0001$, compare to the model group.

gel after centrifugation was observed. The results show that the TPM–NCs–gel exhibited no stratification and remained in a uniform state, indicating good stability and uniformity.

3.6.5. Determination of gel strength, hardness, and adhesion value

The results are shown in Table 5. The strength, hardness, and adhesion value of TPM–NCs–gel were not significantly different from those of the blank gel, indicating that the addition of TPM–NCs suspension had no significant effect on the texture of the blank gel, and the preparation had good coating ductility and strong adhesion.

3.7. Determination of MIC and MBC

As shown in Table 6, the MIC and MBC of the TPM–NCs–gel are smaller than those of the TPM gel. The results indicated that after TPM was prepared as NCs, the particle size decreases, the specific surface area increases and the antibacterial effect is enhanced.

3.8. Determination of bacteriostatic zone

As shown in Table 7, the antibacterial ability of TPM prepared as NCs exhibits enhanced activity. The concentration of the TPM–NCs–gel was positively correlated with the activity of *Staphylococcus aureus*. The antibacterial zone increased with the concentration of the TPM–NCs–gel, and the antibacterial effect was concentration dependent.

3.9. Efficacy evaluation of TPM–NCs–gel

3.9.1. Body weight changes of mice

Body weight can directly reflect the effect of drugs on mice. As shown in Fig. 4, the body weight of mice after modeling first decreased and then increased relative to that of the blank group, possibly because of the loss of appetite caused by modeling. These effects influenced the body weight of the mice. When the mental state of the mice recovered, they began to eat normally, and their weight increased steadily. The mice show no

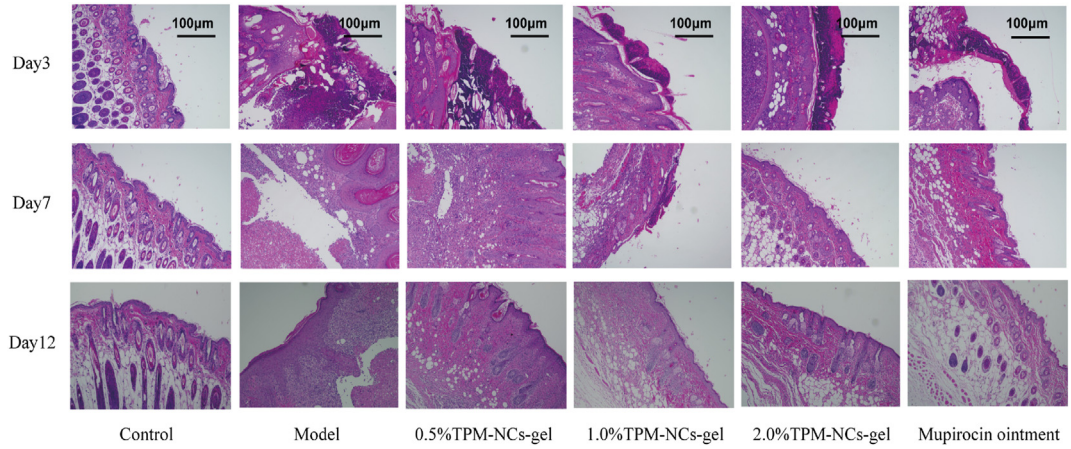

Fig. 7. Typical H&E staining micrographs of the skin of different groups on day 3, day 7 and day 12 (× 10).

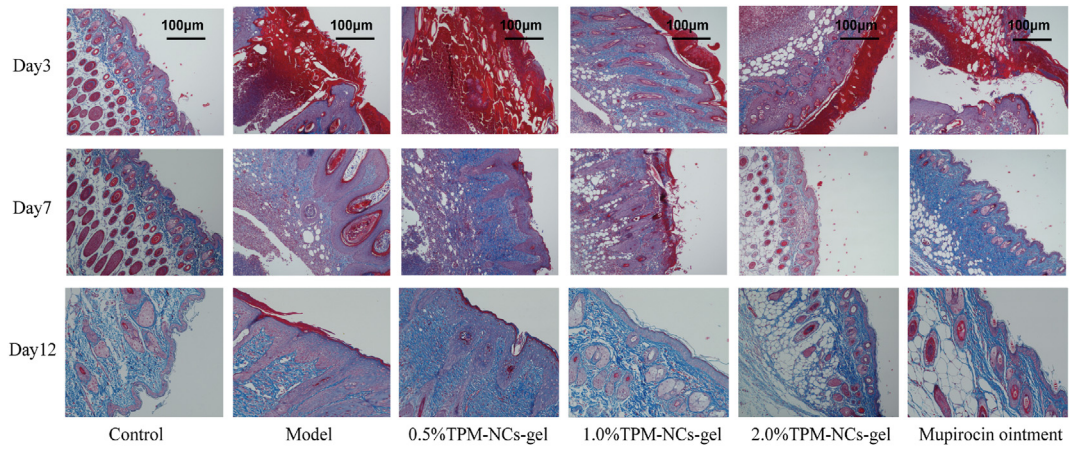

Fig. 8. Typical Masson staining micrographs of the skin of different groups on day 3 (× 10), day 7 (× 10) and day 12 (× 20).

significant difference from the control group.

3.9.2. Skin bacterial load

As shown in Fig. 5, the amounts of bacteria in the skin of the mice in each group gradually decreased over time. Fig. 6 shows the bacterium-carrying capacity of the mouse abscess sites at different periods. When the number of bacterial colonies in the plate was 30–300, it had statistical significance, and when the number of bacterial colonies was less than 30, no statistics were performed.[24] The 2.0% TPM–NCs–gel experimental and positive drug groups had only a small number of bacteria in the diseased skin extract after 7 days of administration.

3.9.3. Skin histopathological sections

As shown in Figs. 7 and 8, *Staphylococcus aureus* infection severely damaged the skin structure of the mice, and pus was observed under the skin. The structure of each skin layer was difficult to distinguish, and a large number of inflammatory cells were infiltrated. After treatment with TPM–NCs–gel and Mupirocin ointment, inflammatory cells gradually decreased, skin structure was remodeled, hair follicles and sebaceous glands appeared, and skin healing was better than that in the model group.

4. Discussion

Log P represents the proportion of drug distribution in the oil and water phases and is an important physicochemical parameter for evaluating drug permeability. The lipophilicity and hydrophilicity of a drug increase with the Log P value. The ideal drug Log P value is 1.0–2.0, and the oil–water distribution coefficient of TPM in different systems is within this range.[25,26] This result indicates good biofilm permeability.[27] TPM is almost insoluble in pure water or normal saline, perhaps because TPM contains a benzene ring structure, the benzene ring is a group composed of 6 carbons, which is lipophilic and less water-soluble. Thus, it exhibits low bioavailability and a poor absorption effect.

The experiment adopted a high-pressure homogenization method to prepare TPM–NCs, which are simple to use. The particle size of TPM can be easily reduced.[28] A single-factor test was conducted, using particle size as the evaluation index. The amount of surfactant, drug, and mannitol was selected as the influencing factors of the TPM–NCs particle size. The Box–Behnken response surface method was used to optimize the formulation process for the TPM–NCs, and the prescription was verified. The results showed that the actual value only slightly deviated from the predicted value, indicating that the model obtained by Box–Behnken response surface method was significant and reliable, and the particle size of the TPM–NCs was basically consistent within the prediction. TPM prepared as an NCs showed improved drug dissolution rate, and NCs had large specific surface areas, which could increase the contact surface between drugs and biofilm and improve bioavailability.[16]

HEC is a non-ionic water-soluble polymer material, which has the characteristics of non-toxicity, non-irritation, and good biocompatibility.[29] When HEC–HHX was used as the substrate, the prepared TPM–NCs–gel was uniform, delicate, and easy to spread, and the measured gel adhesion value was high, indicating that the candidate drug can be easily attached to a skin surface and provide continuous efficacy. The PDI of TPM–NCs–gel was less than 0.3, and the absolute value of Zeta potential was greater than 30 mV, indicating that the particle size distribution was concentrated and the stability was good.[30–33]

Rafael A′ lvarez-Chimal et al. found that antibacterial activity increases as the particle size of the zinc oxide nanoparticles decreases.[34] This effect can be attributed to increased specific surface area, which facilitates full contact between a drug and microorganisms. In addition, antibacterial activity is enhanced. MIC and MBC can reflect the strength of antibacterial ability of drugs, and the smaller the value, the stronger the drug effect.[35,36] In the *in vitro* antibacterial experiment, the MIC and MBC of the TPM–NCs–gel are smaller than those of the TPM gel. TPM prepared as an NCs has a small particle size, leading to the increased specific surface area. These effects enable a drug to have full contact with *Staphylococcus aureus*, destroy the bacterial structure, and enhance the antibacterial effects.

In the *in vivo* antibacterial experiment, the 2.0% TPM–NCs–gel skin bacteria load was less than that of the other experimental TPM–NCs–gel groups after 7 days of treatment. After 12 days of treatment, the 2.0% TPM–NCs–gel group showed no bacteria in the skin, whereas a small number of bacteria still survived in the remaining two groups, suggesting that the therapeutic effect of the TPM–NCs–gel on subcutaneous abscess was concentration dependent. The 2.0% TPM–NCs–gel can effectively remove bacteria in the abscess, and thus the skin tissue structure was remodeled earlier and healing was better than those in the model group, indicating that the 2.0% TPM–NCs–gel and Mupirocin ointment could remove *Staphylococcus aureus* in the subcutaneous abscess quickly and had a considerable bactericidal effect.[37]

5. Conclusion

TPM, which is an insoluble candidate drug, was prepared into a TPM–NCs–gel in this study. The prepared TPM–NCs–gel not only showed an enhanced antibacterial activity *in vitro* but also showed a good therapeutic effect on subcutaneous abscess induced by *Staphylococcus aureus* in mice, especially in the high concentration group of 2% TPM–NCs–gel. This study provides an important reference with significance for the subsequent development and application of TPM as an antibacterial drug.

CRediT authorship contribution statement

Quanwei Xie: Writing – review & editing, Writing – original draft, Visualization, Software, Methodology, Investigation, Formal analysis, Data curation, Conceptualization. **Feirong Zhou:** Writing – review & editing, Writing – original draft, Visualization, Software, Methodology, Investigation, Formal analysis, Data curation, Conceptualization. **Runan He:** Writing – review & editing, Visualization, Software, Methodology, Investigation, Formal analysis. **Lianbao Ye:** Writing – review & editing, Writing – original draft, Validation, Supervision, Resources, Funding acquisition. **Zonghao Lin:** Writing – review & editing, Writing – original draft, Validation. **Xiangyu Nie:** Writing – review & editing, Supervision. **Yuanzheng Wei:** Writing – review & editing, Supervision, Resources, Funding acquisition. **Chuqin Yu:** Writing – review & editing, Supervision, Resources, Funding acquisition, Conceptualization.

Data availability statement

All data can be obtained from the corresponding authors upon a rational request.

Funding

This research was funded by Department of Science and Technology of Guangdong Province and the Guangdong Provincial Academy of Chinese Medical Sciences (2016A020226038), Guangdong Province Higher Education Innovation Team (2024KCXTD035), Guangdong Pharmaceutical University's "Discipline Training Excellence, Innovation and Quality Improvement" Engineering Team Project (NO. 2024ZZ05), Linzhi City Science and Technology Plan Project (2023YZ01).

Declaration of interest statement

No potential conflict of interest was reported by the author(s).

Appendix A. Supplementary data

Supplementary data to this article can be found online at https://doi.org/10.1016/j.jhip.2025.02.004.

References

1. Zhang L, Li Y, Jian F, et al. Role of GraSR in promoting vancomycin resistance in vancomycin-intermediate *Staphylococcus aureus* through MurC. *J Chongqing Med Univ*. 2024;49(10):1067–1073.
2. Zhou Y, Liu H, Zhao Y, et al. Research progress on staphylococcal virulence factors phenol-soluble modulins. *Microbiol Bull*. 2022;49(3):1158–1166.
3. Pitt ME, Nguyen SH, Duarte TPS, et al. Evaluating the genome and resistome of extensively drug-resistant *Klebsiella pneumoniae* using native DNA and RNA nanopore sequencing. *GigaScience*. 2020;9(2):giaa002.
4. Horn J, Stelzner K, Rudel T, et al. Inside job: *Staphylococcus aureus* host-pathogen interactions. *Int J Med Microbiol*. 2018;308(6):607–624.
5. Liu S, She P, Li Z, et al. Insights into the antimicrobial effects of ceritinib against *Staphylococcus aureus in vitro* and *in vivo* by cell membrane disruption. *AMB Express*. 2022;12(1):150.
6. Tarín-Pelló A, Suay-García B, Pérez-Gracia MT. Antibiotic resistant bacteria: current situation and treatment options to accelerate the development of a new antimicrobial arsenal. *Expert Rev Anti Infect Ther*. 2022;20(8):1095–1108.
7. Mittal N, Tesfu HH, Hogan AM, et al. Synthesis and antibiotic activity of novel acylated phloroglucinol compounds against methicillin-resistant *Staphylococcus aureus*. *J Antibiot (Tokyo)*. 2019;72(5):253–259.
8. Lin H, Liu X, Shen Z, et al. The effect of isoflavaspidic acid PB extracted from *Dryopteris fragrans* (L.) schott on planktonic and biofilm growth of dermatophytes and the possible mechanism of antibiofilm. *J Ethnopharmacol*. 2019;241:111956.
9. Shi W. *Research on Phloroglucinol Derivatives and Their Antibacterial Active of Hypericum Curvisepalum*. Tarim Univ; 2020.
10. Shi P. *Synthesis and Biological Activity of Flavaspidic Acid and Albaspidin Compounds*. Guangdong Pharm Univ; 2020.
11. Kalepu S, Nekkanti V. Insoluble drug delivery strategies: review of recent advances and business prospects. *Acta Pharm Sin B*. 2015;5(5):442–453.
12. Wei Q, Wu H, Bu R, et al. Progress in the preparation and quality evaluation of nanoformulations using wet media milling technology. *J Liaocheng Univ*. 2024;37(6):78–86.
13. Ran Q, Wang M, Kuang W, et al. Advances of combinative nanocrystal preparation technology for improving the insoluble drug solubility and bioavailability. *Crystals*. 2022;12(9):1200.
14. Wang Y. *Study on the Construction of Oral Nanocrystal-Loaded Lipid Carriers and the Oral Absorption Promoting Mechanism of BCS-IV Drug Etoposide*. Jilin Univ; 2021.
15. Qiu J. *Preparation of Florfenicol Nanocrystals and Preliminary Study on Bacteriostasis of its Combination with Total Flavonoids from Canarium Pimela Leenh Leave*. Guangdong Pharm Univ.; 2021.
16. Singhal M, Baumgartner A, Turunen E, et al. Nanosuspensions of a poorly soluble investigational molecule ODM-106: impact of milling bead diameter and stabilizer concentration. *Int J Pharm*. 2020;587:119636.
17. Torraga MGF, Giudici R. Stabilizer-free dispersion copolymerization monitoring by in-line NIR spectroscopy. *Ind Eng Chem Res*. 2020;59(35):15497–15505.
18. Liu X. *Study on Nimodipine Nanosuspensions Prepared by Wet Milling and Evaluation of its Bioavaliability*. Tianjin Univ.; 2021.
19. Zhang Q, Wang X, Xue H, et al. Determination and comparison of the solubility, oil-water partition coefficient, intestinal absorption, and biliary excretion of carvedilol enantiomers. *AAPS PharmSciTech*. 2021;22(1):43.
20. Rodrigues TC, Gois IB, Fernandes RPM, et al. Chemical characterization and antimicrobial activity of essential oils from *Croton grewioides* baill. accessions on the phytopathogen xanthomonas campestris pv. campestris. *Pestic Biochem Physiol*. 2023;193:105454.
21. de Morais MC, de Oliveira Lima E, Perez-Castillo Y, et al. Synthetic cinnamides and cinnamates: antimicrobial activity, mechanism of action, and in silico study. *Molecules*. 2023;28(4):1918.
22. Fu G. *Preparation and Evaluation of Relugolix Nanosuspensions for Improved Oral Bioavailability*. Nanchang Univ.; 2023.
23. Chen Y. Research on the effect of TPGS modified mupirocin-silver complex on skin drug-resistant *Staphylococcus aureus* infection. *Bengbu Med Coll*. 2022.
24. Lin Q. *Epidemiological Investigation and Treatment of Pathogenic enterococcus Faecalis Infection from Sheep in Baoding Area*. Hebei Agricult Univ.; 2022.
25. Wang Y. *Preparation of Dihydromyricetin Self-Microemulsion Delivery System and its Pharmacodynamics*. Jiangsu Univ.; 2022.
26. Liu H, Xu S, Tang Z, et al. Study on physicochemical properties of the components of Qinqifeng decoction. *J Chin Mater Med*. 2020;45(12):2858–2864.
27. Li F. *Preparation of Nimodipine Ophthalmic Ointment and Study on its Systemic Transport*. Anhui Univ Chin Med.; 2019. MA thesis.
28. Yu C, Tang W, Zhang B, et al. Preparation and *in vitro* transdermal study of dipalmitoyl hydroxyproline nanostructured lipid carrier and its gel. *J Chin Pharm*. 2022;57(24):2108–2117.
29. Huang J. *Study on the Construction and Composite Mechanism of Hydroxyethyl Cellulose Based Multifunctional Films*. Shanxi Univ Sci and Technol; 2023. PhD dissertation.
30. Shaikh MS, Kale MA. Formulation and molecular docking simulation study of luliconazole nanosuspension–based nanogel for transdermal drug delivery using modified polymer. *Mater Today Chem*. 2020;18:100364.
31. Wang S, Shi Y, Ma J, et al. Enhanced intradermal delivery of Dragon's blood in biocompatible nanosuspensions hydrogel patch for skin photoprotective effect. *J Cosmet Dermatol*. 2023;22(3):1046–1062.
32. Li L. *Heparin-iron Targeting Glycocalyx-Erythrocyte Lifespan axis Ameliorates Renal Anemia in Mice*. Shandong Univ.; 2021. MA thesis.
33. Liu M. *Pr. Eparation of Citral Nanoemulsion and its Application in Citrus Film Coating for Preservation*. Southwestern Univ.; 2022. MA thesis.
34. Chimal Rafael Álvarez, García Pérez Víctor I, Marco Antonio Álvarez Pérez, et al. Influence of the particle size on the antibacterial activity of green synthesized zinc oxide nanoparticles using dysphania ambrosioides extract, supported by molecular docking analysis. *Arab J Chem*. 2022;15(6):103804.
35. Okla MK, Alatar AA, Al-Amri SS, et al. Antibacterial and antifungal activity of the extracts of different parts of *Avicennia marina* (Forssk.). *Vierh Plants (Basel)*. 2021;10(2):252.
36. Hao Y. *Preparation and Antibacterial Properties of Multisite N-Halamine Antibacterial Nanocomposites*. Jilin Univ.; 2022. MA thesis.
37. Qian W, Yan C, He D, et al. pH-triggered charge-reversible of glycol chitosan conjugated carboxyl graphene for enhancing photothermal ablation of focal infection. *Acta Biomater*. 2018;69:256–264.